

Zenith and Azimuth Angle Dependence of Extensive Air Shower Thickness

Davoud Purmohammad^{*1} · Sayed Mohiadin Ataei²

¹ Physics Department, Imam Khomeini International University, Qazvin, Postal Code 3414896818, Iran;

email: purmohammad@sci.ikiu.ac.ir

² Department of Physics, Faculty of Education, Faryab University, Afghanistan;

email: muhiddinataei1368@gmail.com

Abstract. The arrival time distribution of simulated extensive air shower particles, for $10^{14} - 10^{16}$ eV showers initiated by protons, for the observation level of the ALBORZ-I array in Tehran, has been investigated. Using the standard deviation of the time distribution as an indicator of the shower thickness, and defining appropriate observation zones on the ground, we found an asymmetry in the shower thickness of slanted showers. It seems that the early parts in the shower front are thicker than the late parts. A misinterpretation of the thickness of slanted shower fronts in an other research has been corrected. Implications for improvement of accuracy in the shower axis direction estimation have been discussed.

Keywords: Extensive Air Showers, Cosmic Rays, Time Distribution

1 Introduction

Cosmic Rays (CR) are messengers from violently high energy phenomena in the sky. They have been studied since the beginning of the 20th century, by a variety of detection techniques. At energies more than 10^{12} eV, the flux of CR is so low that they can not be practically observed with a single detector smaller than a few meter in size. However, these very high energy particles can produce a huge swarm of particles, mainly electrons¹ and muons, when they enter the atmosphere. The phenomenon is called extensive air shower (EAS). A common method of observing an EAS is to use an array of charged particle detectors laid in a wide area on the ground. Any coincidence of particle detection in several detectors of such an array is due to passage of an EAS in the area. In such a coincidence event, difference in detection times of detectors can be utilized for estimation of direction of arrival of the primary cosmic ray. An EAS can be depicted as a collection of particles in a plane, called shower front, which is normal to the shower axis. The axis is an extension of the primary particle's path in the atmosphere. Since the production of the secondary particles in an EAS occurs as a result of stochastic processes, the shower front is not a sharp thin plane. In fact, the shower front is more like a partial spherical layer with a varying thickness. This thickness is a measure of spatial distribution of the secondary particles in a direction normal to the shower front, and is manifested by a dispersion of arrival times of the particles in a detector. As detection times are used for estimation of the shower axis direction, any time dispersion will affect the accuracy of the estimated direction. Few experiments have tried to measure the arrival time distribution of the EAS particle [1]. More

¹In this paper we use this word for both positrons and electrons.

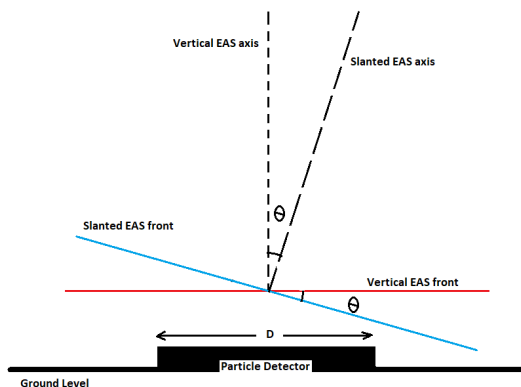


Figure 1: A simplified depiction of a vertical and a slanted extensive air shower front.

statistically reliable results have been obtained by using Monte Carlo simulation techniques. Recently, Bahmanabadi et al. [2] have reported the results of such simulations for arrival time distributions of EAS particles. Their results show the dependence of the shower thickness to the shower core distance, and the shower energy. However, they have misinterpreted some of their results which concerns variation of the shower thickness with the zenith angle of the arrival direction of the EAS. Attention should be paid to the geometrical effect of shower zenith angle on the arrival time distribution. In Figure 1, two planes representing two shower fronts, one with a vertical axis, and the other with an slanted axis are depicted. Since the detector lies on a horizontal surface, the arrival time dispersion of particles in the vertical shower is only dependent on the longitudinal distribution of particles. If all particles move on a thin plane, they will arrive at the detector simultaneously. On the other hand, the same particles moving on a thin slanted surface will not arrive at the same time, and would have a time distribution whose breadth depends on the width of the detector D , and the zenith angle of the shower axis θ . It can easily be shown that for a set of particles uniformly distributed on the plane, the arrival time would have a uniform distribution with $\mu \simeq \frac{D}{2c} \sin \theta$ and $\sigma \simeq \frac{\mu}{\sqrt{3}}$ as its mean and standard deviation respectively, in which c is the speed of light. For a detector of width $D = 1$ m, this would produce only a dispersion of $\sigma \simeq 0.5$ ns for a $\theta = 30^\circ$ shower. For a detection area of width $D \sim 100$ m, the time dispersion would be $\sigma \sim 50$ ns for the same shower. As Bahmanabadi et al. [2] used annular regions with different inner and outer radii, from 5 m to 250 m, on a horizontal observation level, the aforementioned geometric effect has made a huge impact on their arrival time spread for slanted showers. That is the reason for the very large values (a few hundred ns) represented in their Figure 9. On the other hand, rather than moving on a thin front plane, shower particles are distributed along a direction normal to the plane. This would cause an extra delay in the arrival times. Hence, even the particles of a vertical shower will not arrive simultaneously at the ground. Here, we report the results of our analysis on the arrival time spread of simulated shower particles in several regions in the shower front, which are suitably chosen to demonstrate the variation of shower thickness with the core distance, and azimuth angle, for slanted showers of different zenith angles.

2 Simulation of extensive air showers

In this work, CORSIKA(v. 7.35) [3] simulation code has been used for generation of extensive air showers. QGSJET II-04 model [4] for the high energy, and GHEISHA model [5] for the low energy hadronic interactions has been selected. In order to compare our results with the aforementioned work, and apply them for accuracy estimation of the ALBORZ-I array [6], we have used the same input values implemented by Bahmanabadi et al. [2], which are, 1200 m above sea level for the observation level, 0.3 GeV and 0.003 GeV energy threshold for muons and electrons respectively. Since we wanted to concentrate on the impact of shower zenith angle on the shower thickness, we content our self to use only protons as the primary particles for the generation of the EASs. Shower energies were 10^{14} , 10^{15} , and 10^{16} eV. For each of these energies, eight zenith angles, $\theta = (0, 10^\circ, 20^\circ, 30^\circ, 40^\circ, 50^\circ, 60^\circ, 70^\circ)$ were used. The simulated showers had a $\phi = 0$ azimuth angle, i.e. their primary particles arrive from the south. In 10^{14} and 10^{15} eV runs, 100 showers were generated for each zenith angle. In 10^{16} eV runs only 20 showers for each zenith angle were produced. In order to investigate the impact of azimuth angle of the shower, an additional set of 300 showers with $E = 10^{15}$ eV, $\theta = 40^\circ$, and $\phi = (90^\circ, 180^\circ, 270^\circ)$ were also simulated. An extra set of simulation has been made for 300 showers with $E = 3 \times 10^{14}$ eV, and zenith angles $\theta = 0, 25^\circ, 45^\circ$, in order to reproduce the results similar to those depicted in Figure 9 of reference [2] for showers initiated by protons. In total 2280 showers has been generated in 30 CORSIKA runs.

3 Analysis method

In order to observe properties that are location dependent, one can divide the observation level to small zones. This has been done in other researches, for example by observing the particle distributions in different shower core distance intervals. Such annular regions are suitable if one needs to know the variation of an observable property with core distance. However, when shower axis is not vertical, shower particles will have different path lengths, hence different arrival times, at different parts of the same annular region. To avoid mixing the data from such different regions, we tried square zones of the same size at several places at the observation level. The center of the zone no. 1 has been chosen at the shower core. The position of 13 such observation zones is depicted in Figure 2. The center of zones are placed in 0, 45 m, 95 m, and 145 m distances from the shower core. Most of our simulated showers had zero azimuth angle for the primary particles, which according to the CORSIKA standards, these showers arrive from south. For these showers the southern region of observation level receives the earliest particles. In order to investigate the difference in the arrival time distribution in the early and late parts of the shower front, we placed the observation zones along the south-north (x) and east-west (y) axis. For reduction of geometric effect on the arrival time distribution, the size of an observation zone must be as small as possible. Although such a small zone can collect enough particles in the shower core, this is not the case in the farther regions. At first, we used zones of 10 meter radial, and 40° azimuthal width [7]. The results were not useful because the arrival times in the zones at east and west had more geometrical dispersion than the south and north zones. Also, the geometrical effects grow with core distance. Then, we used square zones of 10 meter sides. In this case, the zones were not wide enough to collect so many particle. When we tried $20 \times 20 m^2$ zones, there were more than 10 particles in all zones even in the showers of 50° zenith angle and 10^6 GeV energy. The 10^6 GeV is almost the energy of the best performance for the Alborz-1 array [6]. After trying different sizes, we chose a square of 20 m side as an observation zone. For each shower, the arrival times of electrons and muons

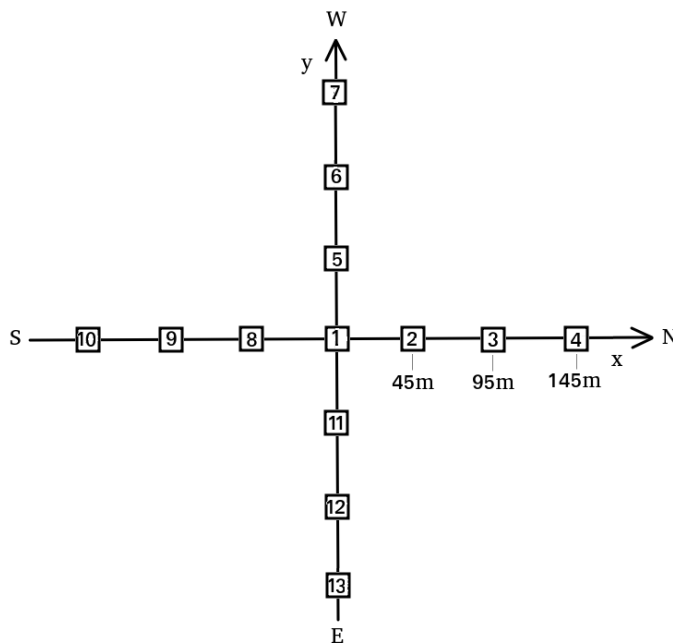


Figure 2: Position of 13 observation zones on the ground. The axes are along south-north and east-west direction as in the CORSIKA code. The center of zone 1 is at the origin. The distances of centers of zones 2, 3, and 4 from origin are 45 m, 95 m, and 145 m respectively. The other corresponding zones are at similar distances. The width of a zone is 20 m.

at each zones have been extracted. Then, the arrival time of the first particle in the shower front is subtracted from arrival time of each particle. In this way, the time distribution for charged particles of each shower has been obtained, with 1 ns bin sizes. The average arrival time distribution is then obtained by adding all the distributions, bin by bin, and dividing the results by the number of showers in a run. An example of average arrival time distribution in the 13 observation zones for a set of 100 showers of 10^{16} eV energy, with a zenith angle of $\theta = 40^\circ$, and azimuth of 0° (arriving from south) is shown in Figure 3. As we can see, the earliest zone for such a shower front is the zone no. 10 which covers an interval of (135 m, 155 m) from the shower core in the south, and the latest zone is no. 4 at the same distance in the north. To demonstrate the disadvantage of using annular regions for the arrival time analysis, we have also obtained the time distribution for annular regions of the same core distance intervals as zones defined in Figure 2. The results for the arrival time distributions are presented in Figure 4. Here, the $(0, 10)m$ interval corresponds to the zone 1, the $(35, 55)m$ interval corresponds to the zones 2, 5, 8, 11, the $(85, 105)m$ interval corresponds to zones 3, 6, 9, 12, and the $(135, 155)m$ interval corresponds to the zones 4, 7, 10, 13. It is clear that the time dispersions in the annular regions are considerably larger than the corresponding square zones. In fact, the the time distribution in an annular region is a superposition of time distributions of several small zones similar to those defined in Figure 2. For example, the time distribution in the $r \in (135, 155)m$ interval in the Figure 4 is almost a superposition of distributions in the zones 4, 7, 10, and 13 in the Figure 3.

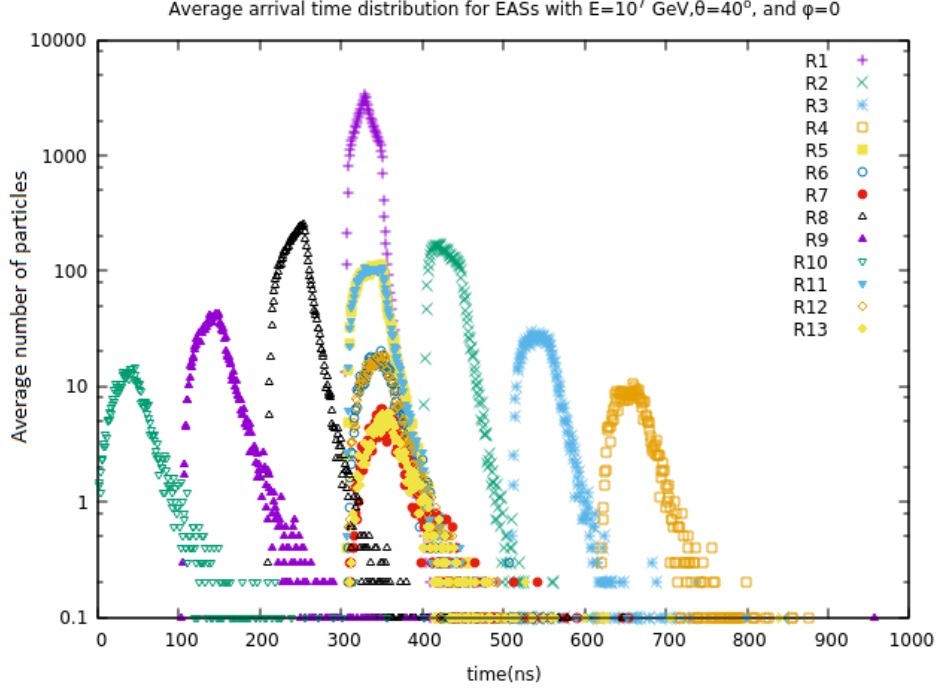


Figure 3: An average particles arrival time distribution for 20 showers with $E = 10^{16}$ eV, $\theta = 40^\circ$, and $\phi = 0^\circ$, i.e. arriving from south, in 13 different regions defined in Figure 2

Although we tried to optimize the size of the zones, for the lowest energy showers in our work ($E = 10^{14}$ eV), number of particles in zones other than the five in the center was very low ($N < 20$). In this research, we were interested in the dispersion in the arrival time distribution in each zone. The standard deviation of the distribution is a suitable measure of the dispersion:

$$\sigma^2 = \frac{\sum_{i=1}^n N_i (t_i - \tau)^2}{\sum_{i=1}^n N_i} \quad (1)$$

in which $n = 1000$ is the number of time bins, N_i is the number of particles in the i th bin, and $t_i = i$ ns is the time of the bin because the bin size is 1 ns. τ is the mean of the distribution:

$$\tau = \frac{\sum_{i=1}^n N_i t_i}{\sum_{i=1}^n N_i} \quad (2)$$

The observed time dispersion is a combination of the pure geometric dispersion σ_g , discussed in section 1, and a dynamic dispersion σ_d originated from random interactions of secondary particles: $\sigma = \sqrt{\sigma_g^2 + \sigma_d^2}$. The values for σ_g , which only depends on the shower zenith angle, and the size of the detector, is given for several zenith angles with $D = 20$ m, in table 1.

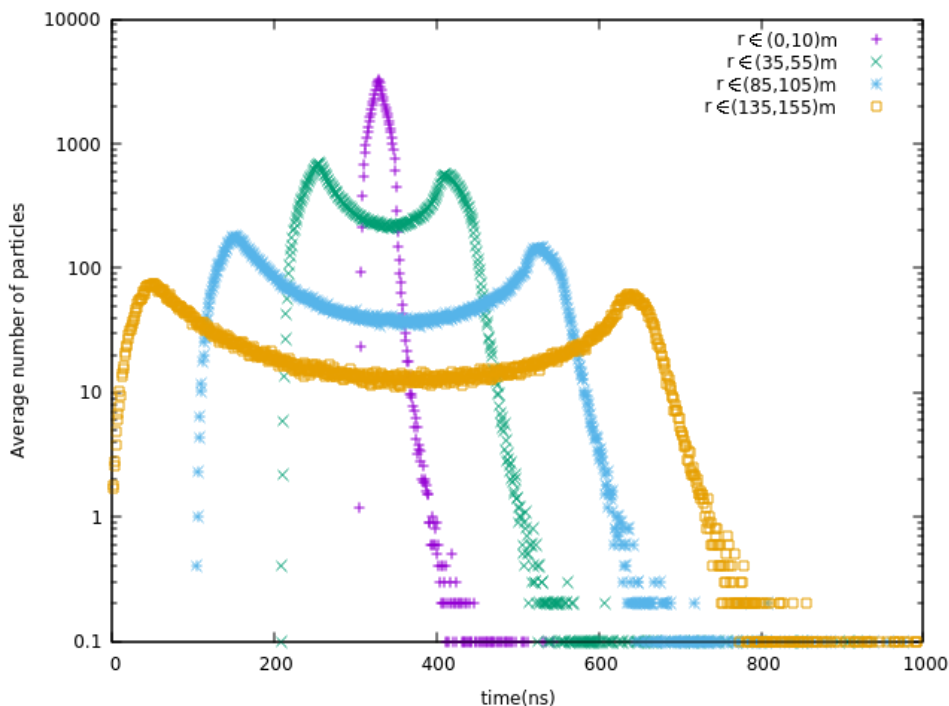


Figure 4: An average particles arrival time distribution for 20 showers with $E = 10^{16}$ eV, $\theta = 40^\circ$, and $\phi = 0^\circ$, i.e. arriving from south, in four different annular regions of core distance intervals similar to the zones defined in Figure 2. Here, the $(0,10)m$ interval corresponds to the zone 1, the $(35,55)m$ interval corresponds to the zones 2, 5, 8, 11, the $(85,105)m$ interval corresponds to zones 3, 6, 9, 12, and the $(135,155)m$ interval corresponds to the zones 4, 7, 10, 13.

4 Results and discussion

Our results show that the time dispersion, which can be called shower thickness, varies with core distance, shower zenith angle as well as shower energy. In Figure 5, the variation of the shower thickness with shower zenith angle for different primary energies at a few selected zones are presented. All of these showers had zero azimuth angle, which means they arrived from south. Since showers with zenith angles $\theta = 60^\circ$ and 70° had very low number of particles we have excluded them from the analysis. All thickness values are considerably higher than corresponding σ_g . Since $\sigma_g = 0$ for vertical showers, an estimation of σ_d is directly obtained from the data of $\theta = 0$ points. Figure 5a shows that at the zone 1, near the shower core, for 10^6 and 10^7 GeV showers, the shower thicknesses are very close to those obtained by geometric effects (see Table 1). The dynamic dispersion is more important than the geometric one at zone 1 for 10^5 GeV showers with zenith angles greater than 40° . For 10^5 GeV showers with 50° zenith angle, there is not enough particles at zones other than zone 1. For all zenith angles, these low energy showers have not enough particles at zone 4 which is at 145 m core distance. The 10^5 GeV showers of 40° zenith angle have not enough particles in zone 12 which is at 95 m core distance. That is the reason for the lack of corresponding data points in Figure 5. For higher energy showers and at larger core distances, Figure 5b

Table 1: Geometric arrival time dispersion for showers of different zenith angles in an area of $D = 20m$ width.

θ°	$\mu(ns)$	$\sigma_g(ns)$
0	0	0
10	6	3.5
20	11.5	6.5
30	17	10
40	21.5	13
50	25.5	15
60	29	17.5
70	31.3	19

to 5d, the dynamical aspects become more important. Hence, at the zone 4 (Figure 5d), 145 m away from the core, a decrease of thickness with the zenith angle is observed. While the thickness seems to mildly decrease with the shower energy at the core, it increases with the energy at farther core distances. Since each box in the Figure 5 corresponds to a different core distance, one can see that the shower thickness at the highest core distance in this work, which is $\langle r \rangle = 155m$, is less than 30 ns. Had we used annular regions, like those mentioned in Figure 4, we would obtained higher values for the shower time dispersion. In Figure 6, results for the estimated time dispersions of $E = 3 \times 10^{14}eV$ showers with three different zenith angles, in four annular regions are presented. The results indicate the increase in the time dispersion with core distance for slanted showers. The showers used for Figure 6 are similar to those used by Bahmanabadi et al. [2] in their Figure 9, and our results are compatible with theirs. To indicate the compatibility of our results with reference [2], we repeated the analysis for the aforementioned showers in 5 meter core intervals, from the shower cores to a maximum distance of 250 meter. The results, presented in Figure 7, indicate the compatibility. Although the time dispersions in annular regions in slanted showers are considerably higher than those for square regions of 20 m length, we can not consider them as an indicator of shower thickness. Our results show some difference in the shower thickness at different sides of the shower front. It seems that at the south side, which our simulated shower front hits the ground earlier, the thickness is slightly higher than the north side, which is the latest side of the shower front. Figure 8 compares the variation of the shower thickness with the zenith angle at different cardinal directions of 10^7 GeV showers. Although the variation in the shower thickness at different directions is negligible at 45 m core distances, the south-north thickness difference is higher at farther regions. The average difference is around 5 ns in the 95 m and up to 9 ns in the 145 m core distances for showers with zenith angles higher than $\theta = 20^\circ$. This difference has to be related to the atmospheric depth difference between the early and the late sides of the shower front. The earliest part of the shower front passes through the shortest distance in the atmosphere, hence suffers less absorption. More particles are absorbed in the air at the latest side of the shower front. This would result in a more energetic population in the late part of the front, in which less time dispersion is expected. In the early part of the front, the number of low energy particles is higher than the later parts, and since low energy particles are slower than high energy ones which reach the ground first, the time distribution is more disperse in the earlier parts. In order to exclude the possible impact of the azimuth angle of the shower axis on the early-late difference in the shower thickness, a set of simulations for $E = 10^6$

GeV showers with $\theta = 40^\circ$ zenith angle and $\phi = 0, 90^\circ, 180^\circ, 270^\circ$ azimuth angles has been carried out. These angles correspond to showers arriving from north, west, south, and east, respectively. In Figure 9, variation of the shower thickness with the azimuth angle for these showers at the zones of 95 m and 145 m core distances is presented. In all the cases, the latest part of the shower front has less thickness than the earliest part. Since the statistical error bars in Figure 9 overlap one another, the values of σ_s and their errors are given in the table 2.

5 Conclusion

By investigating the arrival times of EAS particles for simulated showers generated from cosmic ray protons of 10^{14-16} eV, we found a small asymmetry in the shower thickness in slanted showers. The asymmetry can be quantified as $A = 2 \frac{\sigma_{early} - \sigma_{late}}{\sigma_{early} + \sigma_{late}}$, in which σ_{early} , and σ_{late} are thickness of shower front at early and late sides respectively. An example is presented in table 3 for thicknesses at 95 meter core distance of 10^6 GeV showers of 40° zenith angle. A misinterpretation for the shower thickness of slanted EASs found by Bahmanabadi et al. [2] has been corrected, by choosing appropriate observation zones. Our results show that the shower front is thinner at the late side of the front. For an array of detectors which register a sample of shower particle arrival times, used for estimation of shower axis direction, this implies a more accurate timing at detectors which lie at the later part of the array. This will improve the accuracy of estimated shower axis direction. We can use the formula given in the reference [8]:

$$\Delta\theta = \sqrt{2} \left[2 \left(\frac{c\Delta s}{d} \right)^2 + \frac{1}{2} \left(\frac{\Delta d}{d} \right)^2 \sin^2 \theta \right]^{1/2} \quad (3)$$

for the error in the estimated shower direction, in which $\Delta s = \sigma$ is the error in the arrival time of the shower front, d is the distance between adjacent detectors, Δd is the width of a detector, and θ is the shower zenith angle. Thus, in the case of the central cluster of ALBORZ-I array [9] which consists of 5 detectors with $\Delta d = 0.5$ m and $d = 5$ m, for $\theta = 30^\circ$, the error in shower direction in the late part is 2° lower than early part for 45 m core distance. This difference is about 30° at 95 m core distance. Although the amount of the early-late difference in the front thickness is as low as a few nano-seconds in the core distances of 100-150 m, it is worth to investigate it at larger core distances for more energetic EASs, as those observed by AUGER observatory.

Acknowledgment

Most of the computation in this work has been performed with the HPC supercomputer of Imam Khomeini International University. We are grateful to the manager and the staff of HPC facility of IKIU for their support. The authors thank the anonymous reviewers for their valuable comments.

References

- [1] Aielli, G., et al. 2012, Nucl. Instrum. Methods Phys. Res., Sect. A, 661, S50.
- [2] Bahmanabadi, M., & Mortazavi Moghadam, S. 2018, New Astron. , 61, 5.

Table 2: Values of σ and their statistical errors for showers with energy $E = 10^6$ GeV and zenith angle $\theta = 40^\circ$ arriving from cardinal directions, as observed at different sides of the shower core, at two core distances.

Core Distance (m)	ϕ°	Shower arrives from	Observation point at	$\sigma(ns)$	$\Delta\sigma(ns)$
95	0	South	South	20.1	1.4
95	0	South	East	21.3	2.1
95	0	South	West	19.4	1.9
95	0	South	North	18.4	1.4
95	90	East	South	19.6	1.9
95	90	East	East	21.2	1.4
95	90	East	West	18.3	1.4
95	90	East	North	20.9	2.0
95	180	North	South	18.2	1.4
95	180	North	East	21	1.9
95	180	North	West	20.4	1.8
95	180	North	North	21.4	1.4
95	270	West	South	21	1.9
95	270	West	East	18.1	1.3
95	270	West	West	20.5	1.3
95	270	West	North	20.9	1.9
145	0	South	South	22.3	2.5
145	0	South	East	23.1	3.8
145	0	South	West	22.4	3.8
145	0	South	North	19.3	2.4
145	90	East	South	22.2	3.6
145	90	East	East	22.6	2.4
145	90	East	West	18.9	2.4
145	90	East	North	22.2	3.5
145	180	North	South	19.7	2.4
145	180	North	East	23.9	3.6
145	180	North	West	23.4	3.6
145	180	North	North	22.4	2.4
145	270	West	South	21	3.3
145	270	West	East	19.1	2.3
145	270	West	West	22.5	2.3
145	270	West	North	22	3.4

Table 3: A measure of early-late asymmetry in shower thickness for showers with energy $E = 10^6$ GeV and zenith angle $\theta = 40^\circ$ arriving from cardinal directions, as observed at 95 meter core distance.

Shower arrives from	$A = 2 \frac{\sigma_{early} - \sigma_{late}}{\sigma_{early} + \sigma_{late}}$
South	0.09 ± 0.10
East	0.15 ± 0.09
North	0.16 ± 0.09
West	0.12 ± 0.09

- [3] Heck, D., et al. 1998. CORSIKA: A Monte Carlo Code to Simulate Extensive Air Showers. Report FZKA 6019. Forschungszentrum, Karlsruhe; available from http://www-ik.fzk.de/corsika/physics_description/corsika_phys.html.
- [4] Kalmykov, N. N., et al. 1997, Nucl. Phys. B (Proc. Suppl.), 52, 17.
- [5] Fesefeldt, H. 1985, The Simulation Of Hadronic Showers-Physics and Applications. Report No. PITHA-85/02. RWTH, Aachen.
- [6] Abdollahi, S., et al. 2016, Atropart. Phys., 76, 1.
- [7] Ataei, S. M. 2019, Investigation of azimuthal asymmetry in the time distribution of extensive air showers by Monte carlo simulation, Master Thesis, Imam Khomeini International University, Qazvin, Iran.
- [8] Bahmanabadi, M., et al. 2002, Exp. Astron., 13, 39.
- [9] Bahmanabadi, M., & Heydarizadeh, M. 2019, Nucl. Instrum. Methods Phys. Res., Sect. A, 932, 62.

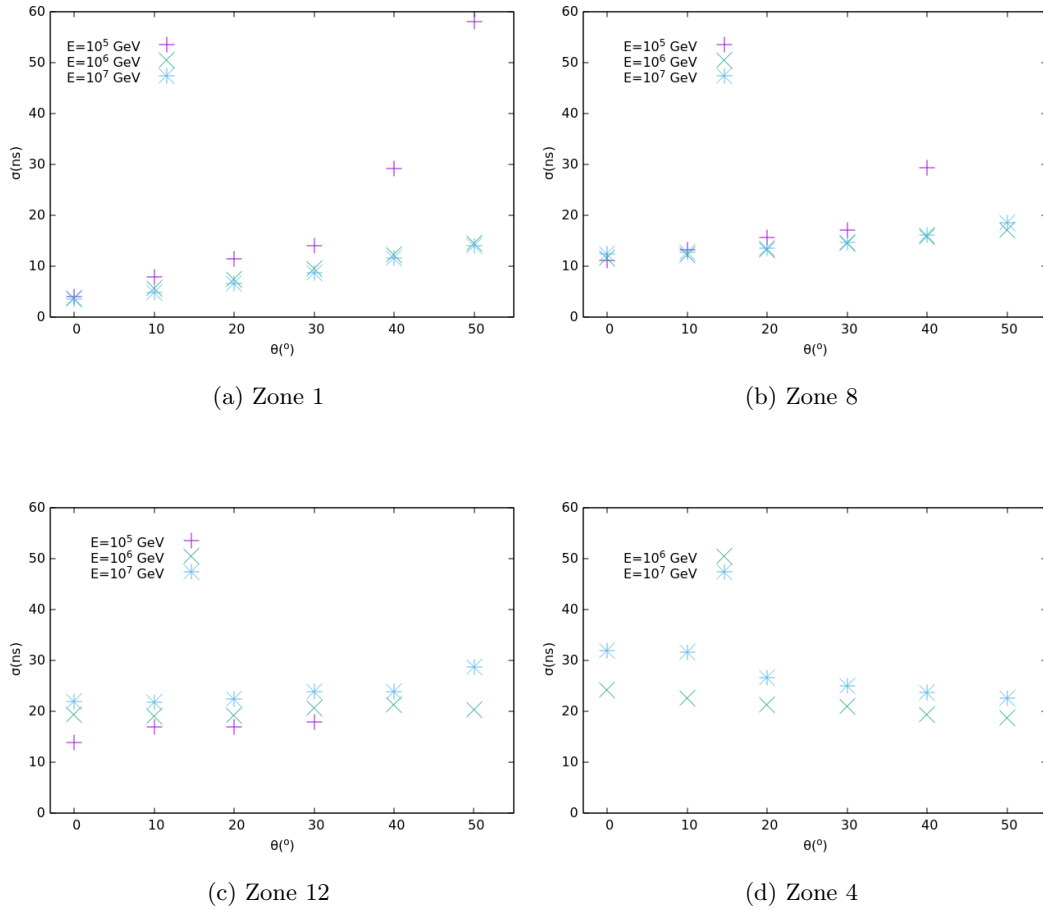


Figure 5: Variation of the shower thickness with the zenith angle for EASs of zero azimuth angle (arriving from south), and different energies at 4 selected observation zones. Figure 5a is for the zone 1 which is at the core of the showers. Figure 5b is for the zone 8 which its center is at 45 m distance in the south of the shower core. Figure 5c is for the zone 12 which its center is at 95 m distance in the east of the shower core. Figure 5d is for the zone 4 which its center is at 145 m distance in the north of the shower core.

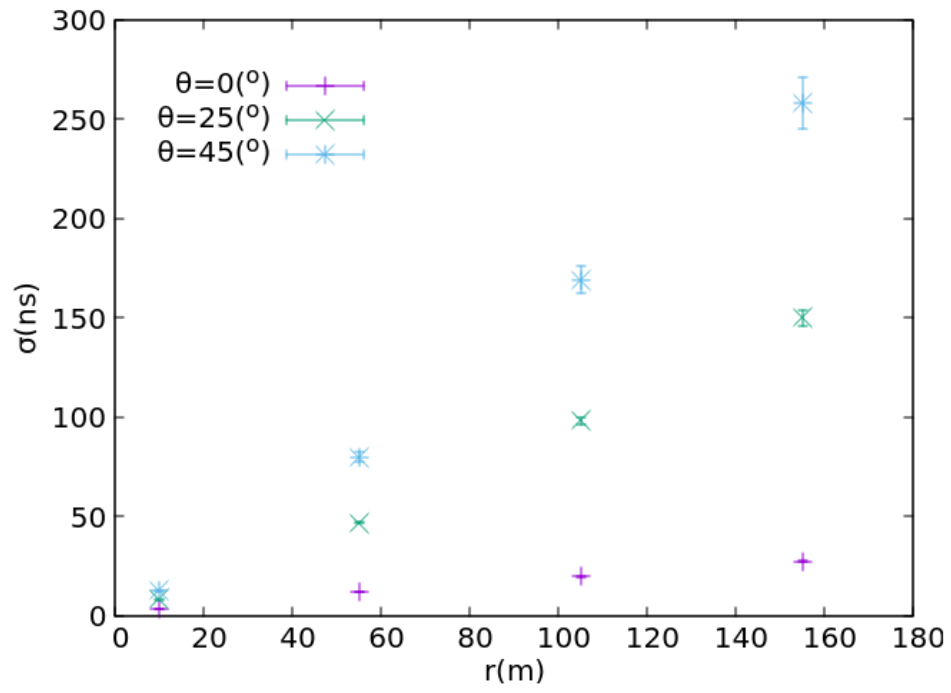


Figure 6: Variation of shower thickness with core distance, for annular regions with different core distances correspond to zones defined in Figure 2, for showers of $E = 3 \times 10^{14} eV$ energy and $\theta = 0, 25^\circ, 45^\circ$. Each point is an average for 100 showers. Vertical error bars are statistical errors.

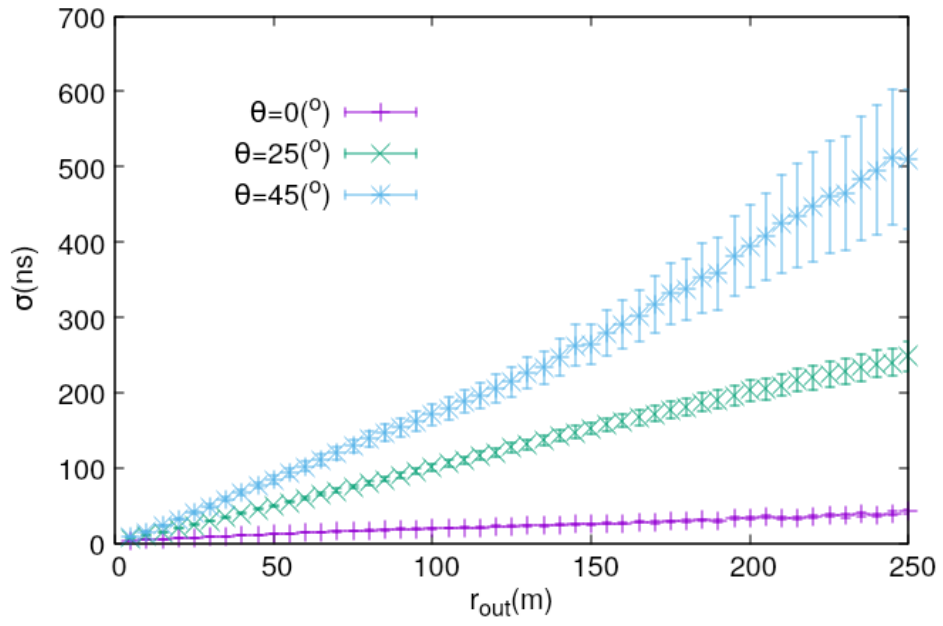
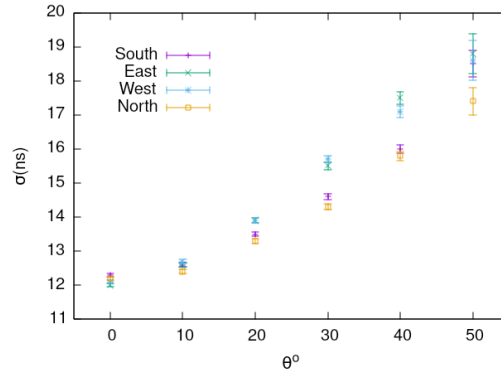
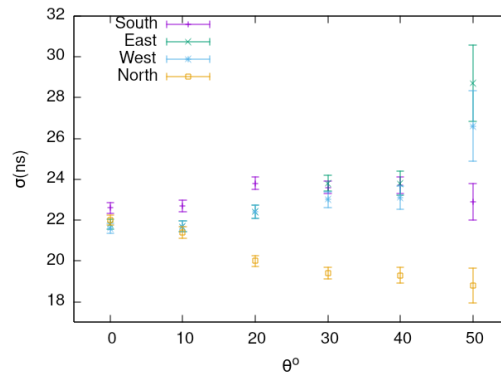


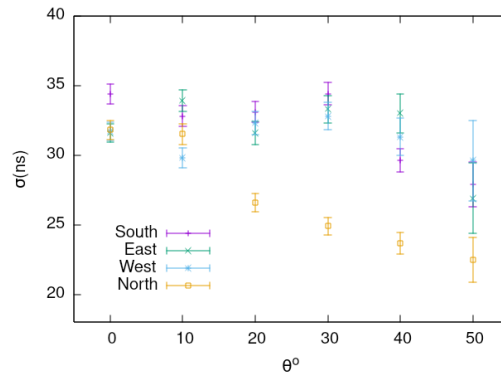
Figure 7: Variation of shower thickness with core distance, for annular regions of 5m core distance interval, for showers of $E = 3 \times 10^{14} eV$ energy and $\theta = 0, 25^\circ, 45^\circ$. Each point is an average for 100 showers. Vertical error bars are statistical errors.



(a)



(b)



(c)

Figure 8: Variation of shower thickness with the zenith angle for $E = 10^7$ GeV showers, all arriving from south ($\phi = 0^\circ$), in 3 core distances and 4 cardinal directions on the ground: (a) for 45 m, (b) for 95 m, and (c) for 145 core distances.

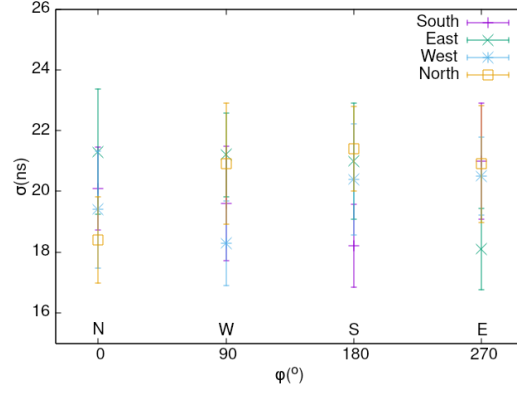
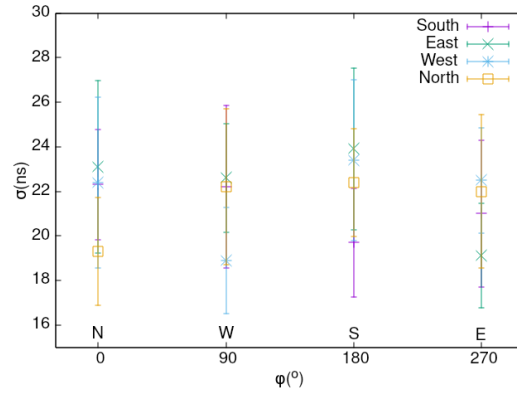
(a) $\langle r \rangle = 95$ m(b) $\langle r \rangle = 145$ m

Figure 9: Variation of the shower thickness with shower axis azimuth angle, in the zones at different directions for showers of energy $E = 10^6$ GeV and zenith angle $\theta = 40^\circ$. ϕ is the azimuth angle of shower axis, defined as the angle between the north direction and the projection of the primary cosmic ray momentum on the ground. The cardinal direction signs on the abscissa specify the direction which the shower is going. Figure (a) is for 95 m, and Figure (b) for 145 m core distances.